# ADHESION AND DEBONDING IN A MODEL OF ELASTICS STRING

G. M. COCLITE, G. FLORIO, M. LIGABÒ, AND F. MADDALENA

Abstract. We consider a 1D semilinear wave equation (and the corresponding initial boundary value problem of Neumann type) modeling the dynamics of an elastic string. We include a source term modeling the interaction of the string with a rigid substrate by an adhesive layer. This force is characterized by a jump to zero when a critical value of the displacement is reached. We obtain conditions for the initial value problem in order to guarantee the regularity of the solution and the adhesion phenomenon. Finally, we consider a regularization of the source term and numerically analyze the problem. We study the qualitative properties of the solutions for different initial conditions.

## 1. Introduction

Mathematical modeling of phenomena in life sciences and manufacturing engineering is a difficult task due to the complexity of the underlying physical mechanisms involved. Growth, fracture and wetting [1, 2, 3, 4] are examples of this kind of problems. In particular, the problems related to adhesion and debonding are extremely important because of their applications [5], for instance in the delamination phenomenon in laminated composite materials [6]. Costitutive models on the adhesive materials have to be assumed in order to analyze the mechanical systems. For instance, rigorous approaches (based on the calculus of variations) to the *static* problem of adhesion in elastic thin structures under various constitutive assumptions on the adhesive material have been performed in [7, 8, 9, 10]. On the other hand, the analysis of the evolution requires the use of multidimensional hyperbolic equations involving mathematical issues not yet well understood.

In this paper we address a prototypical *dynamical* problem by studying the adhesion of an elastic string glued to a rigid substrate. We will assume a discontinuous softening behavior of the adhesive material, i.e. the adhesive stress jumps to zero when a critical value of the displacement is reached. It is interesting to notice that the choice of a costitutive model for the adhesive layer is fundamental an must be carefully considered. For instance, it has been shown in [11] that a discontinuity in the source term, like the one previously mentioned, can induce non-trivial consequences: it is possible to build explicit examples with solutions that exhibit instability under different regularizations of the source term. Thus, we want to extend the analysis performed in [11].

The paper is organized as follow. In Section 2 we present the initial boundary problem and the costitutive model for the adhesive layer. In Section 3 we obtain the conditions that must be imposed of the initial conditions in order to ensure the regularity of the solutions and guarantee that there is not a debonding phenomenon. In Section 4, after introducing a regularization of the source term, we numerically study the properties of some solutions of the problem. Finally, in Section 5 we draw some conclusions.

---

*Date*: July 28, 2018.

2010 *Mathematics Subject Classification.* 35L05, 74B20, 35J25.

*Key words and phrases.* Adhesion elasticity, wave equation, Neumann boundary conditions.

G. M. Coclite and F. Maddalena are members of the Gruppo Nazionale per l'Analisi Matematica, la Probabilità e le loro Applicazioni (GNAMPA) of the Istituto Nazionale di Alta Matematica (INdAM). G. Florio and M. Ligabò are supported by the Gruppo Nazionale per la Fisica Matematica (GNFM) of INdAM through PROGETTO GIOVANI. G. Florio is supported by INFN through the project QUANTUM and by MIUR through the FABBR research grant.



https://dx.doi.org/10.1016/j.camwa.2019.03.020

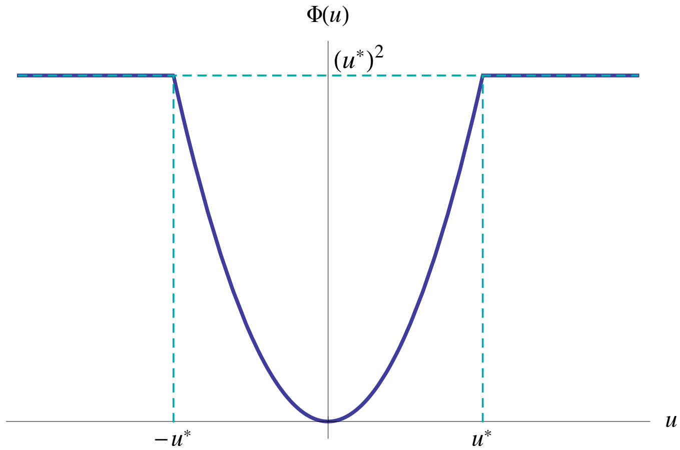


FIGURE 1. Potential $\Phi(u)$ in Eq. (2.2).

## 2. The model

Let us consider a one dimensional material body, i.e. a *string*, whose rest configuration at the initial time $t = 0$ coincides with the interval $[0, L]$ and the displacement field is denoted by

$$u : [0, \infty) \times [0, L] \to \mathbb{R}.$$

We consider the mechanical system with the following energy density:

$$e[u] = \frac{1}{2}\rho(\partial_t u)^2 + \frac{1}{2}K_e(\partial_x u)^2 + \Phi(u), \tag{2.1}$$

where $\rho > 0$ denotes the mass density, $K_e$ denotes the elastic stiffness of the string, and $\Phi(u)$ denotes the adhesion potential modeling the energetic contribution of the glue layer. We assume for the potential $\Phi$ a behavior like in Fig. 1:

$$\Phi(u) = \begin{cases} u^2, & \text{if } |u| \le u^*, \\ (u^*)^2, & \text{if } |u| > u^*. \end{cases} \tag{2.2}$$

This corresponds to a discontinuous softening behavior of the adhesive material: the adhesive stress jumps to zero when a critical value of the displacement (denoted $u^*$) is reached.

The Euler equation associated to the above energy density (2.1) is

$$\rho\partial_{tt}^2 u - K_e \partial_{xx}^2 u = -\Phi'(u), \tag{2.3}$$

equipped with Neumann boundary conditions. For sake of notational simplicity, the mass density $\rho$ and the extensional stiffness $K_e$ are assumed both equal to 1. The string interacts with an underlying rigid support through an infinitesimal layer of adhesive material characterized by an internal energy $u \mapsto \Phi(u)$ with the threshold $u^*$ set to 1.

The balance of momentum delivers the semilinear initial boundary value problem

$$\begin{cases} \partial_{tt}^2 u = \partial_{xx}^2 u - \Phi'(u), & t > 0, 0 < x < L, \\ \partial_x u(t,0) = \partial_x u(t,L) = 0, & t > 0, \\ u(0,x) = u_0(x), & 0 < x < L, \\ \partial_t u(0,x) = u_1(x), & 0 < x < L, \end{cases} \tag{2.4}$$

where $u_0 \in H^1(0,L)$, $u_1 \in L^2(0,L)$ and $\Phi'$ has a jump discontinuity in $u = \pm 1$ such that

$$u \in (-\infty, -1) \cup (1, \infty) \Rightarrow \Phi'(u) = 0,$$
$$0 < u < 1 \Rightarrow 0 < \Phi'(u) \le \lim_{u \to 1^-} \Phi'(u),$$

$$-1 < u < 0 \Rightarrow 0 > \Phi'(u) \geq \lim_{u \to -1^+} \Phi'(u).$$

According to our conventions, we will consider

$$\Phi(u) = \begin{cases} u^2, & \text{if } |u| \leq 1, \\ 1, & \text{if } |u| > 1, \end{cases} \tag{2.5}$$

and

$$\Phi'(u) = \begin{cases} 2u, & \text{if } |u| \leq 1, \\ 0, & \text{if } |u| > 1. \end{cases} \tag{2.6}$$

The energy associated to the problem (2.4) is

$$E(t) = \int_0^L \left( \frac{(\partial_t u(t,x))^2 + (\partial_x u(t,x))^2}{2} + \Phi(u(t,x)) \right) dx. \tag{2.7}$$

## 3. Conditions for adhesion and regularity

A natural question is whether, given certain assumptions on $u_0$ and $E(0)$, it is possible to find a condition such that the adhesion of the string is ensured. Moreover, one would like to find conditions so that the solution is regular. In this section we will tackle this problem. In particular, we will consider dissipative solutions $u$ of the problem (2.4) (see Appendix A) and proof two theorems.

### 3.1. **Adhesion.**

**Theorem 3.1.** *Let $u$ be a dissipative solution of* (2.4)*. If*

$$\|u_0\|_{L^\infty(0,L)} < 1, \qquad E(0) < 1, \tag{3.1}$$

*then*

$$\|u\|_{L^\infty((0,\infty)\times(0,L))} < 1. \tag{3.2}$$

*Proof.* Since $u$ is continuous at least for a short time interval $[0,\tau]$ we have

$$|u(t,x)| < 1, \qquad (t,x) \in [0,\tau] \times [0,L].$$

Define $\tau^*$ as follows

$$\tau^* = \sup \{\tau > 0 \,\text{such that for every}\, (t,x) \in [0,\tau] \times [0,L] \; |u(t,x)| < 1\}.$$

We claim that

$$\tau^* = \infty. \tag{3.3}$$

Observe that

$$\Phi(u(t,x)) = u^2(t,x), \qquad (t,x) \in [0,\tau^*) \times [0,L].$$

Therefore

$$E(t) = \int_0^L \left( \frac{(\partial_t u(t,x))^2 + (\partial_x u(t,x))^2}{2} + (u(t,x))^2 \right) dx, \qquad t \in [0,\tau^*),$$

and, in particular,

$$E(t) \geq \frac{\|u(t,\cdot)\|^2_{H^1(0,L)}}{2}, \qquad t \in [0,\tau^*).$$

Since $u$ is dissipative, using the Sobolev embedding $H^1(0,L) \subset L^\infty(0,L)$ (see [**?**, Theorem 8.5]), we have

$$\|u(t,\cdot)\|^2_{L^\infty(0,L)} \leq \frac{\|u(t,\cdot)\|^2_{H^1(0,L)}}{2} \leq E(t) \leq E(0) < 1, \qquad t \in [0,\tau^*),$$

that proves (3.3) □

### 3.2. Regularity.

**Theorem 3.2.** *Let $u$ be a dissipative solution of* (2.4)*. If*

$$u_0 \in W^{2,\infty}(0,L), \tag{3.4}$$

*and there exists a time $\tau$ such that*

$$\operatorname{supp}(u(t,\cdot)) \subset\subset (0,L), \qquad t \in [0,\tau), \tag{3.5}$$

*then*

$$u \in W^{2,\infty}((0,\tau)\times(0,L)), \tag{3.6}$$

$$E(T) = E(0), \qquad 0 \le T < \tau. \tag{3.7}$$

*Proof.* Thanks to (3.5) we can see $u$ as the solution of the Cauchy problem

$$\begin{cases} \partial_{tt}^2 u = \partial_{xx}^2 u - \Phi'(u), & t>0, x\in\mathbb{R},\\ u(0,x) = \widetilde{u}_0(x), & x\in\mathbb{R},\\ \partial_t u(0,x) = \widetilde{u}_1(x), & x\in\mathbb{R}, \end{cases} \tag{3.8}$$

where $\widetilde{u}_0$ and $\widetilde{u}_1$ are the trivial extensions of $u_0$ and $u_1$ to $\mathbb{R}$. Following [11, Section 4.1], using the first order reformulation of the problem and the d'Alembert and the Duhamel Formulas, we have that

$$\partial_x u(t,x) = \partial_x \widetilde{u}_0(x+t), \qquad [0,\tau)\times\mathbb{R}. \tag{3.9}$$

as a consequence

$$\partial_{xx}^2 u \in L^\infty((0,\tau)\times\mathbb{R}). \tag{3.10}$$

Since

$$\partial_{tt}^2 u = \partial_{xx}^2 u - \Phi'(u)$$

we have also

$$\partial_{tt}^2 u \in L^\infty((0,\tau)\times\mathbb{R}). \tag{3.11}$$

Clearly, (3.10) and (3.11) imply (3.6).

Finally, due to (3.6) we can multiply the equation in (3.8) by $\partial_t u$ and get (3.7). □

## 4. Numerical examples

In this section we will study the problem (2.4) with different initial conditions in order to analyze the properties of the solutions. As we will see, they exhibit a rich phenomenology. As already stated in the Introduction, it has been shown [11] that the source term of the form (2.6) introduces some problems in the well-posedness of the problem. Therefore, in order to avoid confusion, we will consider a particular class of approximating functions and study the corresponding solutions.

### 4.1. Approximation of $\Phi'$.

Let us consider the approximation

$$\tilde{\Phi}'(u) = u\left(\operatorname{Erf}\left(\frac{u+u^*}{\epsilon}\right) - \operatorname{Erf}\left(\frac{u-u^*}{\epsilon}\right)\right) \tag{4.1}$$

where

$$\operatorname{Erf}(u) = \frac{2}{\sqrt{\pi}}\int_0^u e^{-s^2}ds. \tag{4.2}$$

We show an example of $\tilde{\Phi}'$ in figure 2 where we have fixed $u^* = 1$ and $\epsilon = 10^{-4}$.

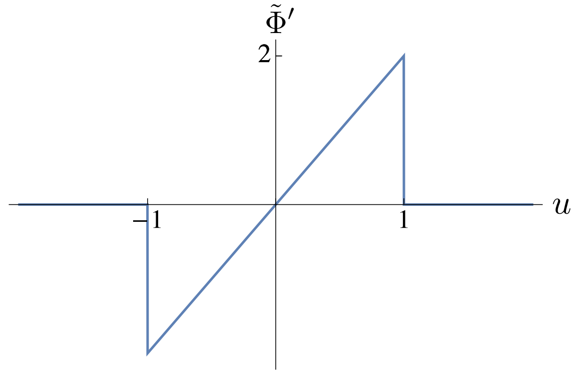


FIGURE 2. Approximation the the source term $\Phi$ in Eq.(4.1) with $u^* = 1$ and $\epsilon = 10^{-4}$.

4.2. **Examples.** In the following examples the numerical integration of the problem (2.4) is performed using the method of lines with a spatial discretization based on a grid ranging from 300 to 1000 points and up to sixth-order finite differences. We have verified that the Neumann boundary conditions are satisfied with an error smaller than $10^{-10}$. We have also tested different values of $\epsilon$ in $\tilde{\Phi}'$. In the examples we have fixed $\epsilon = 10^{-4}$.

**Example 4.1.**

Let us take initial value such that $u(0,x) = u_0(x)$ is in $C^2([0,L])$:

$$\begin{cases} u_0(x) = \xi_0 \left(\frac{x^3}{3} - L\frac{x^2}{2}\right), & 0 \le x \le L, \\ u_1(x) = \xi_1, & 0 \le x \le L. \end{cases} \tag{4.3}$$

In Figures 3 and 4 we plot, respectively, the solution of 2.4 with initial conditions (4.3) and its first order derivatives with respect to time and space coordinates. In the simulation we have used the values $\xi_0 = 0.006$, $\xi_1 = 1.2$, $L = 10$ and a total time evolution $T = 10$. In Figure 3 we have also inserted the plans with $u = \pm 1$ in order to show the regions where the solution has reached and exceeded the critical values. From the results, it is evident that the initial conditions allow a part of the system to pass $u = 1$. It is possible to see that these two values depend on $\xi_0$ and $\xi_1$. On the other hand, the simulations show that the system also exhibits another feature: the debonding process is reversed and $u$ takes values less than 1. The values $t^*$ (time) and $x^*$ (position) where again $u = 1$ and the debonding is reversed are more evident by inspecting the behavior of $\partial_t u$ and $\partial_x u$. Interestingly, $\partial_x u$ is not very sensible to the debonding process.

**Example 4.2.**

We consider initial values such that $u$ is in $C^1([0,L])$ for $t = 0$:

$$\begin{cases} u_0(x) = \xi_0 b\, c(x), & 0 \le x \le L, \\ u_1(x) = \xi_1, & 0 \le x \le L. \end{cases} \tag{4.4}$$

where $b$ is a constant defined as

$$b = \frac{1}{-\frac{1}{4}L\sqrt{4a^2 - L^2} + a^2\left(-\tan^{-1}\left(\frac{L}{\sqrt{4a^2-L^2}}\right)\right) + aL}, \tag{4.5}$$

and

$$c(x) = -\frac{1}{2}x\sqrt{a^2 - x^2} + \frac{1}{2}a^2\tan^{-1}\left(\frac{x\sqrt{a^2-x^2}}{x^2 - a^2}\right) + ax, \quad 0 \le x \le L/2, \tag{4.6}$$

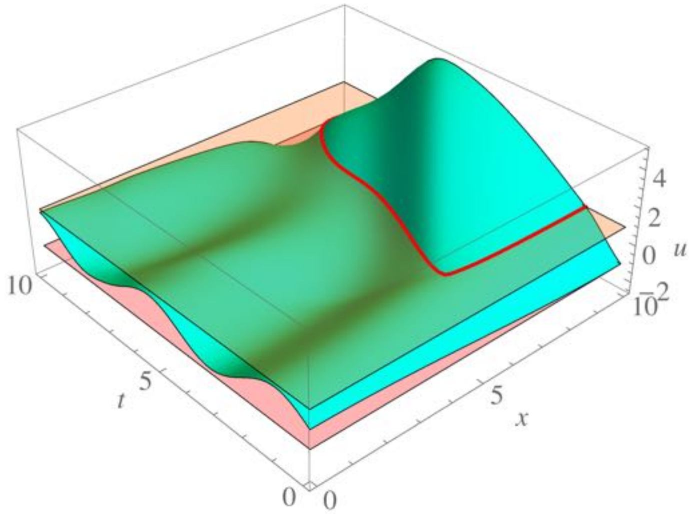


FIGURE 3. Solution of (2.4) with initial conditions (4.3). See text for the numerical values used in the simulation.

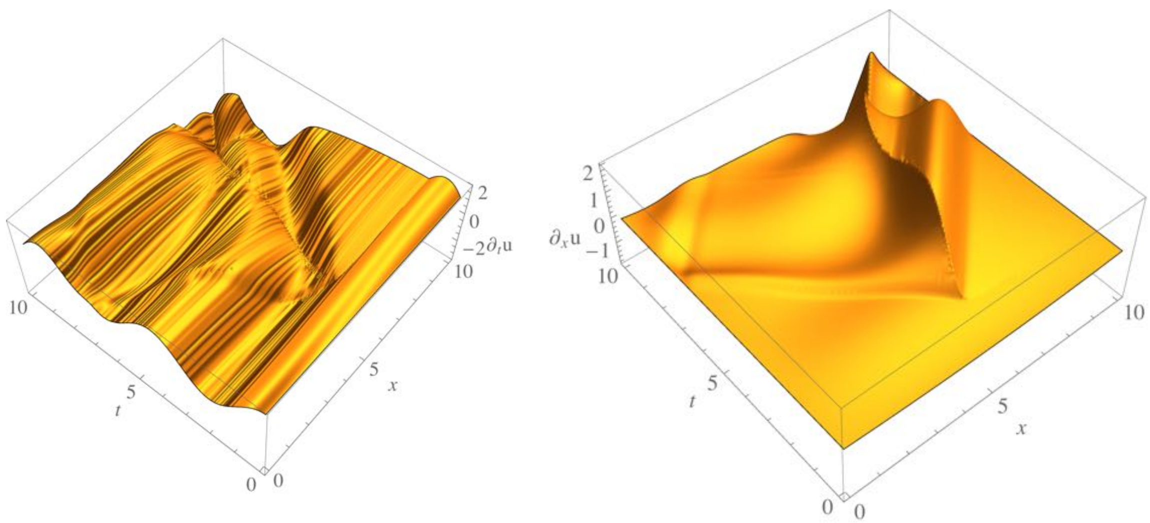


FIGURE 4. Left: derivative with respect to time of $u$ shown in Figure 3. Right: derivative with respect to space of $u$ shown in Figure 3. See text for the numerical values used in the simulation.

$$
\begin{aligned}
c(x) = & -\frac{1}{4}L\sqrt{4a^2-L^2} + a^2\left(-\tan^{-1}\left(\frac{L}{\sqrt{4a^2-L^2}}\right)\right) \\
& + \frac{1}{2}\left((L-x)\sqrt{a^2-(L-x)^2} + a^2\tan^{-1}\left(\frac{L-x}{\sqrt{a^2-(L-x)^2}}\right) + 2ax\right), \quad L/2 < x \le L,
\end{aligned} \tag{4.7}
$$

with $a > L/2$. We notice that the second space derivative of $c$ is not continuous in $x = L/2$. We have performed two different simulations. In Figures 5 and 6 we plot, respectively, the solution of (2.4) with initial conditions (4.4) and its first order derivatives with respect to time and space coordinates. In the simulation we have used the values $\xi_0 = 0.7$, $\xi_1 = 1.1$, $a = 6$, $L = 10$ and a total time evolution $T = 3$. In Figures 7 and 8 we find the solution for the same system but with $\xi_1 = 1.4$. As in the previous example, we observe that the inversion point (where the debonding is reversed) acts as a source for the direct observation of propagation along the characteristics. Moreover, we explicitly

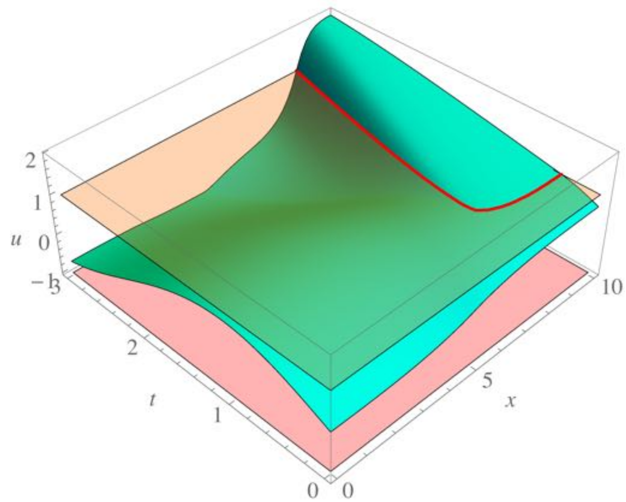


FIGURE 5. Solution of (2.4) with initial conditions (4.4). See text for the numerical values used in the simulation.

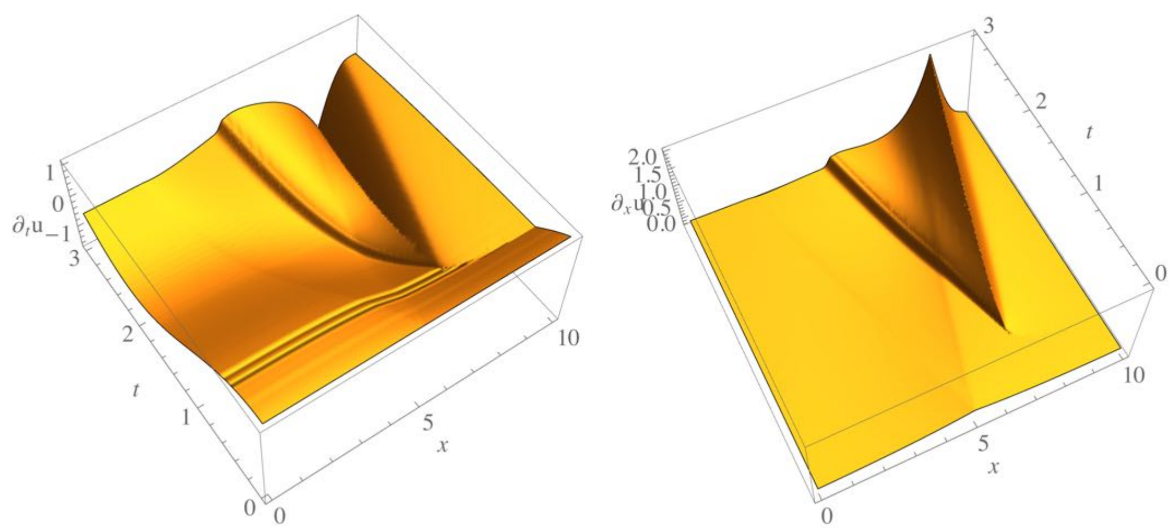


FIGURE 6. Left: derivative with respect to time of $u$ shown in Figure 5. Right: derivative with respect to space of $u$ shown in Figure 5. See text for the numerical values used in the simulation.

observe propagation along the characteristics from the initial point $(t = 0, x = L/2)$ where $\partial_x u$ is not $C^2$. From other numerical experiments (not shown in the paper) we can deduce that this phenomenon is ubiquitous whenever there are two (or more) points in the $x$-domain at $t = 0$ with $\partial_x u$ not in $C^2$.

**Example 4.3.**

We consider now the initial conditions:

$$\begin{cases} u_0(x) = \xi_0(-\frac{1}{2} + b\, c(x)) + 1, & 0 \le x \le L, \\ u_1(x) = \xi_1, & 0 \le x \le L. \end{cases} \tag{4.8}$$

where we have defined $b$ and $c$ in Equations (4.5)-(4.7). Thus, we fix the discontinuity point of the second derivative of $u$ with respect to $x$ (at $t = 0$) when $u(0, L/2) = 1$. Moreover, we set $\xi_0 = 0.7$, $\xi_1 = -1.2$ (the initial velocity is reversed), $a = 6$, $L = 10$ and a total time evolution $T = 3$. As in the

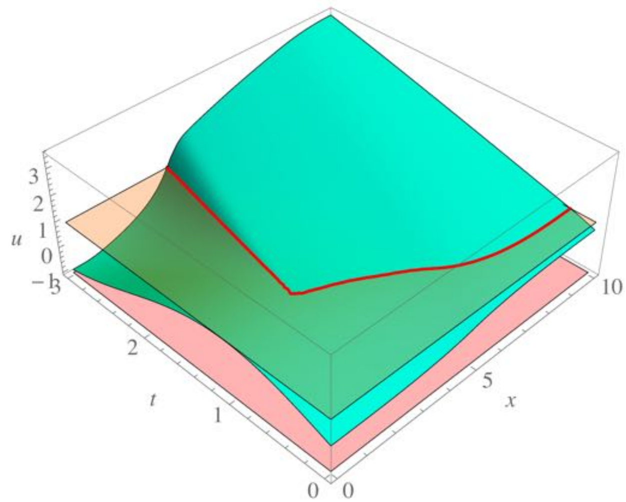


FIGURE 7. Solution of (2.4) with initial conditions (4.4). See text for the numerical values used in the simulation.

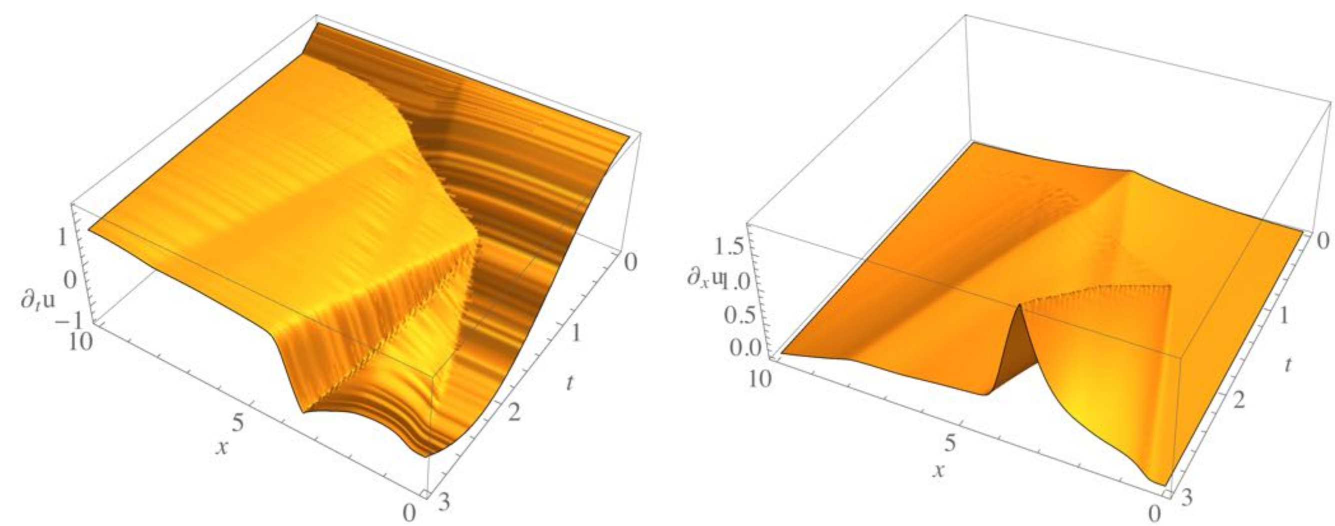


FIGURE 8. Left: derivative with respect to time of $u$ shown in Figure 7. Right: derivative with respect to space of $u$ shown in Figure 7. See text for the numerical values used in the simulation.

previous cases, in Figures 9 and 10 we plot, respectively, the solution of (2.4) with initial conditions (4.8) and its first order derivatives with respect to time and space coordinates. We notice that the point $(t = 0, x = L/2)$ is now both an inversion point and a discontinuity point for the initial second space derivative of $u$. Thus we again observe the explicit propagation along the characteristics. Moreover, the value of $\xi_1$ is large enough to observe a complete debonding phenomenon with $u < -1$ after some time. This is evident form the behavior of $\partial_t u$ in Figure 4.7. We also notice that there are not new sources of characteristics.

We stress that we have numerically tested that separating the inversion point and the discontinuity point gives rise to two separated characteristics sets. This is evident from the results obtained in the following example.

**Example 4.4.**

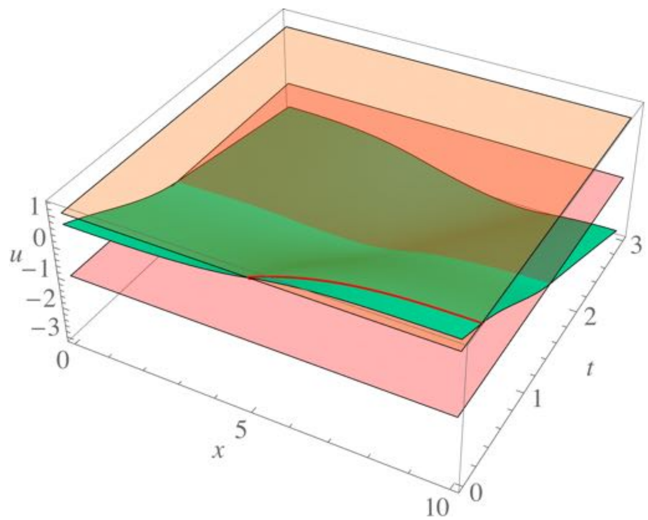


FIGURE 9. Solution of (2.4) with initial conditions (4.8). See text for the numerical values used in the simulation.

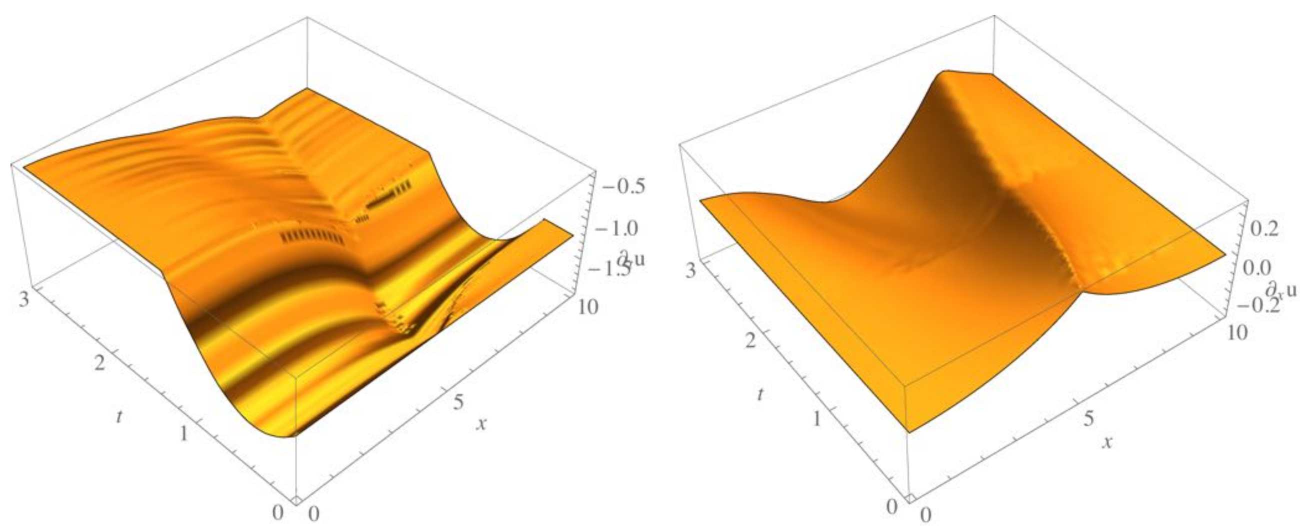


FIGURE 10. Left: derivative with respect to time of $u$ shown in Figure 9. Right: derivative with respect to space of $u$ shown in Figure 9. See text for the numerical values used in the simulation.

Let us consider the initial conditions

$$\begin{cases} u_0(x) = \xi_0(\frac{1}{2} + b\ c(x)), & 0 \le x \le L, \\ u_1(x) = \xi_1, & 0 \le x \le L. \end{cases} \tag{4.9}$$

In Figures 11 and 12 we show, respectively, the solution of (2.4) with initial conditions (4.9) and its first order derivatives with respect to time and space coordinates [same parameters used for the simulations with the conditions in Equation (4.8)]. Moreover, in this case there is not a complete debonding, even in the example where a large negative value of $\xi_1$ has been chosen. As a consequence, we can observe a new set of characteristics in the plots of $\partial_t u$ and $\partial_x u$.

**Example 4.5.**

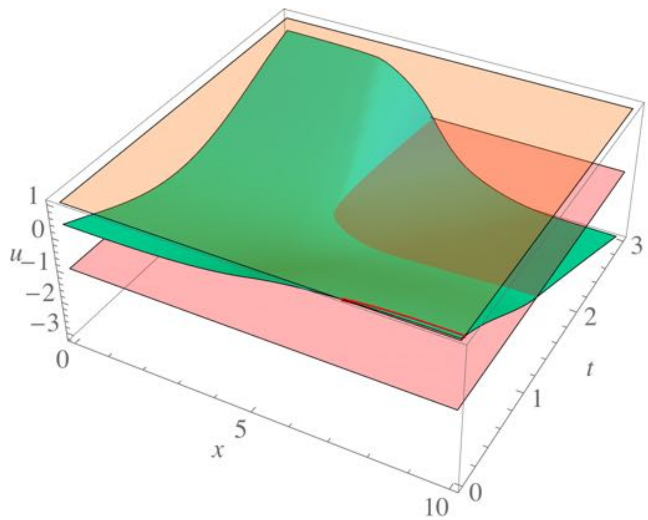


FIGURE 11. Solution of (2.4) with initial conditions (4.9). See text for the numerical values used in the simulation.

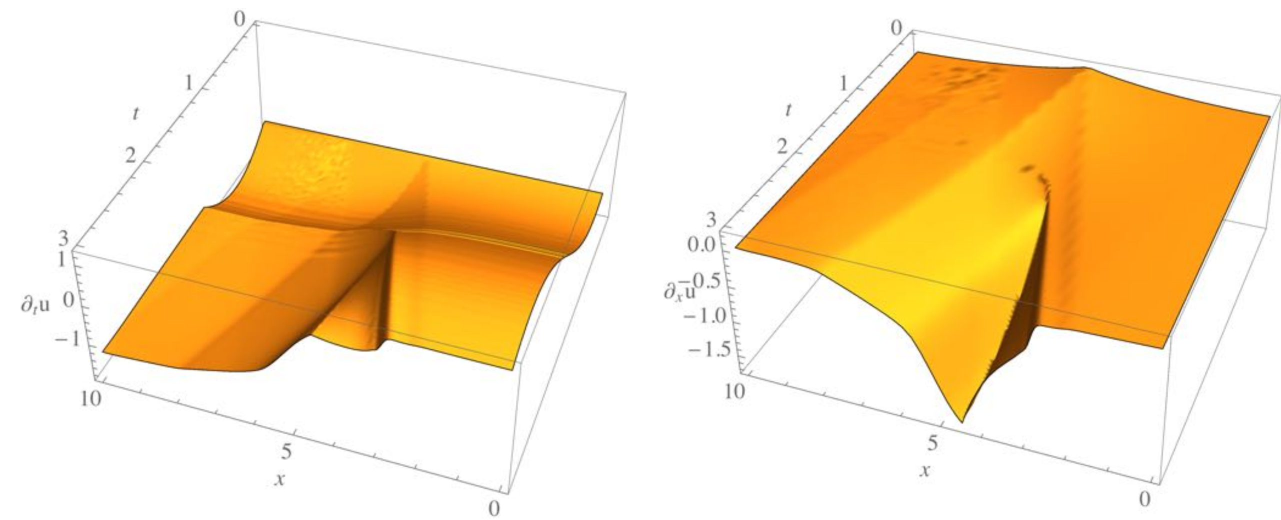


FIGURE 12. Left: derivative with respect to time of $u$ shown in Figure 11. Right: derivative with respect to space of $u$ shown in Figure 9. See text for the numerical values used in the simulation.

We have also considered the case of initial condition where $\partial_t u(0, x) = u_1(x)$ is in $C([0, L])$:

$$\begin{cases} u_0(x) = \xi_0(-\frac{1}{2} + b\, c(x)) + 1, & 0 \leq x \leq L, \\ u_1(x) = \xi_1 b\, \frac{d}{dx}[c(x)], & 0 \leq x \leq L. \end{cases} \tag{4.10}$$

The discontinuity point of the second derivative of $u$ with respect to $x$ (at $t = 0$) appears for $x = L/2$ when $u(0, L/2) = 1$. We have fixed $\xi_0 = 0.7$, $\xi_1 = 0.8$, $a = 6$, $L = 10$ and a total time evolution $T = 3$. In Figures 13 and 14 we show, respectively, the solution of (2.4) with initial conditions (4.10) and its first order derivatives with respect to time and space coordinates. We observe the propagation of the discontiuity in both partial derivatives.

**Example 4.6.**

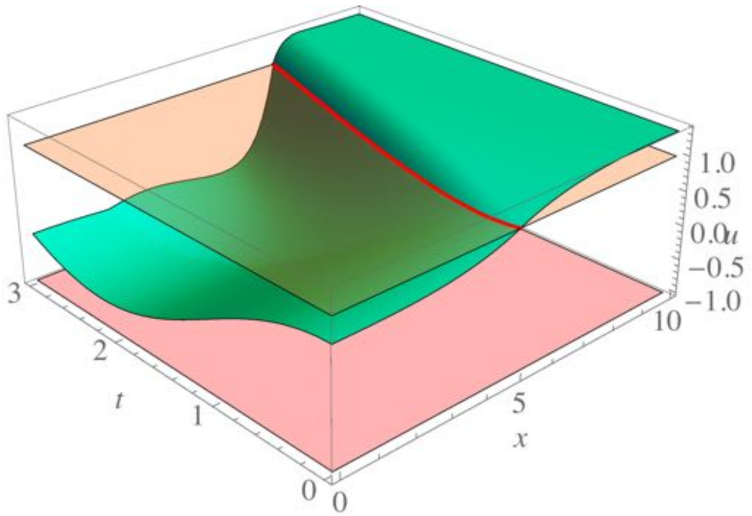


FIGURE 13. Solution of (2.4) with initial conditions (4.10). See text for the numerical values used in the simulation.

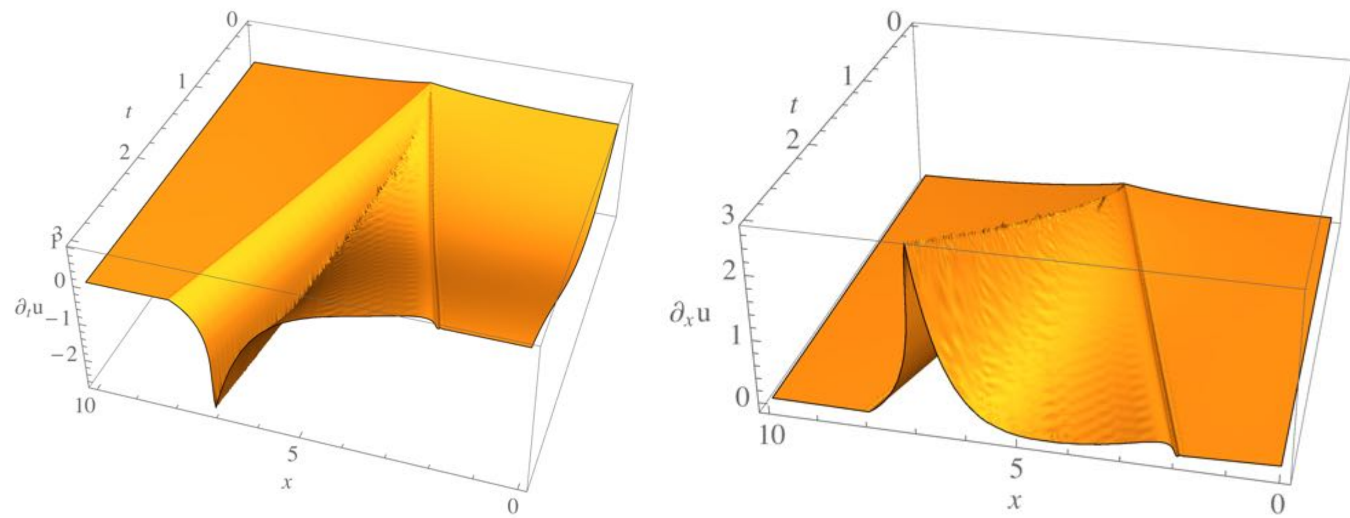


FIGURE 14. Left: derivative with respect to time of $u$ shown in Figure 13. Right: derivative with respect to space of $u$ shown in Figure 13. See text for the numerical values used in the simulation.

Finally, we have considered the case of initial condition where $u$ at $t = 0$ is in $C([0, L])$. In order to perform the numerical simulation we have mollified the initial data in the following way:

$$\begin{cases} u_0(x) = \xi_0 f_\eta(x), & 0 \le x \le L, \\ u_1(x) = \xi_1, & 0 \le x \le L, \end{cases} \tag{4.11}$$

where

$$f_\eta(x) = \frac{2}{\left(\frac{L}{2} - \eta\right) L} \times \begin{cases} x^2, & 0 \le x < \frac{L}{2} - \eta, \\ -\frac{L/2-\eta}{\eta} x^2 + L \frac{L/2-\eta}{\eta} x - L \frac{(L/2-\eta)^2}{2\eta}, & \frac{L}{2} - \eta \le x < \frac{L}{2} + \eta, \\ (x-L)^2, & \frac{L}{2} + \eta \le x \le L, \end{cases} \tag{4.12}$$

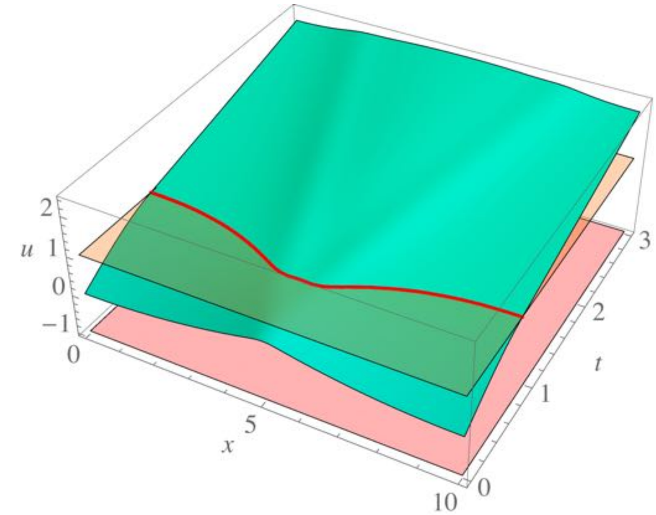


Figure 15. Solution of (2.4) with initial conditions (4.11). See text for the numerical values used in the simulation.

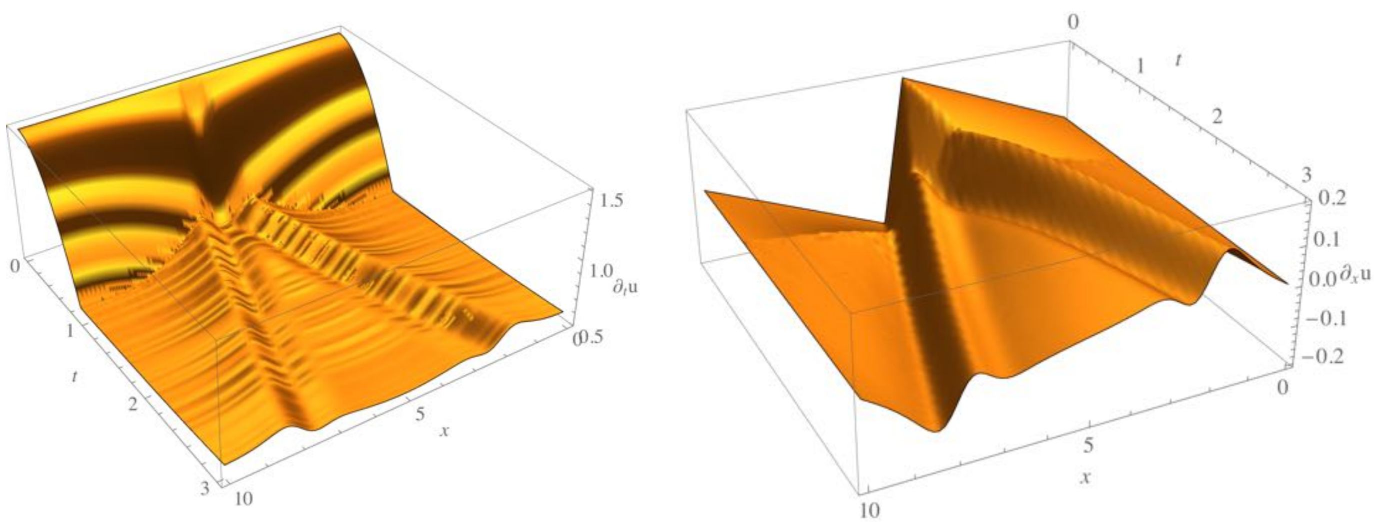


Figure 16. Left: derivative with respect to time of $u$ shown in Figure 15. Right: derivative with respect to space of $u$ shown in Figure 15. See text for the numerical values used in the simulation.

and $\eta$ is the mollification parameter. We have fixed $\xi_0 = 0.5$, $\xi_1 = 1.5$, $\eta = 0.3$, $L = 10$ and a total time evolution $T = 3$. In Figures 15 and 16 we show, respectively, the solution of (2.4) with initial conditions (4.11) and its first order derivatives with respect to time and space coordinates. Also in this case, we directly observe the presence of characteristics due to debonding and an hint of the propagation due to the jump of the value of the first derivative in $t = 0, x = L/2$. We have verified an analogous behavior of the solution $u$ when the value of $\eta$ is reduced.

## 5. Conclusions

In this paper we have considered a prototypical model for the description of adhesion and decohesion phenomena in an elastic string interacting with a rigid substrate by an adhesive layer. The use of a costitutive model based of a source term involving a jump discontinuity introduces some difficulties in the well-posedness for the derivation of solutions of the initial boundary problem. On the other hand, we have been able to obtain conditions ensuring the regularity of these solutions and the possibility to prevent the string to detach from the substrate. Moreover, the numerical analysis of the dynamics has been based on a regularization of the source term. Thus, we have studied different classes of initial conditions and studied their propagation along the characteristics. It is natural to think about extensions of this work using the same costitutive law. One would naturally consider two and three dimensional systems in order to study laminated composite materials. Moreover, the introduction of temperature and, therefore, the adoption of a thermoelastic model would represent an interesting generalization.

## References


[1] A. Goriely, *The Mathematics and Mechanics of Biological Growth*, Springer, 2017.

[2] R. Burridge, J. B. Keller, *Peeling, slipping and cracking some one-dimensional free-boundary problems in mechanics*, SIAM Rev., **20** (1978), pp. 31-61.

[3] P.G. de Gennes, F. Brochard-Wyart, D. Quéré, *Capillarity and wetting phenomena: drops, pearls and waves*, Springer-Verlag, New York, 2004.

[4] K. Kendall, M. Kendall, F. Rehfeldt, *Adhesion of Cells, Viruses and Nanoparticles*, Springer-Verlag, New York, 2011.

[5] R. A. Sauer, *A Survey of Computational Models for Adhesion*, Jour. of Adhesion **92** (2016), pp. 81-120.

[6] F.Shen, K.H.Lee, T.E.Tay, *Modeling delamination growth in laminated composites*, Composites Science and Technology **61** (2001), pp. 1239-1251.

[7] F. Maddalena, D. Percivale, *Variational models for peeling problems*, Int. Free Boundaries, **10** (2008), pp. 503-516.

[8] F. Maddalena, D. Percivale, G. Puglisi, L. Truskinowsky, *Mechanics of reversible unzipping*, Continuum Mech. Thermodyn., **21** (2009), pp. 251-268.

[9] F. Maddalena, D. Percivale, F. Tomarelli, *Adhesive flexible material structures*, Discr. Continuous Dynamic. Systems B, **17** (2012), pp. 553-574.

[10] F. Maddalena, D. Percivale, F. Tomarelli, *Elastic structures in adhesion interaction*, in Variational Analysis and Aerospace Engineering, A. Frediani, G. Buttazzo, editors, Springer Optimization and its Applications, **66** 2012, pp. 289-304.

[11] G. M. Coclite, G. Florio, M. Ligabò, F. Maddalena, *Nonlinear waves in adhesive strings*, SIAM J. Appl. Math., **77** (2017), pp. 347-360.


## Appendix

## Appendix A. Dissipative solutions

Given the problem (2.4), we can define a *dissipative solution* as in the following:

**Definition A.1.** *We say that a function* $u : [0,\infty) \times [0, L] \to \mathbb{R}$ *is a dissipative solution of* (2.4) *if*

(*i*) $u \in C([0,\infty) \times [0, L])$;

(*ii*) $\partial_t u,\ \partial_x u \in L^\infty(0,\infty; L^2(0, L))$;

(*iii*) *for every test function* $\varphi \in C^\infty(\mathbb{R}^2)$ *with compact support*

$$\begin{aligned}\int_0^\infty \int_0^L \left(u\partial_{tt}^2\varphi + \partial_x u \partial_x \varphi + \Phi'(u)\varphi\right) dtdx \\ - \int_0^L u_1(x)\varphi(0,x)dx + \int_{\mathbb{R}} u_0(x)\partial_t\varphi(0,x)dx = 0;\end{aligned} \tag{A.1}$$

(*iv*) *(energy dissipation) for almost every* $t > 0$

$$\begin{aligned}\int_0^L \left(\frac{(\partial_t u(t,x))^2 + (\partial_x u(t,x))^2}{2} + \Phi(u(t,x))\right) dx \\ \le \int_0^L \left(\frac{(u_1(x))^2 + (u_0'(x))^2}{2} + \Phi(u_0(x))\right) dx.\end{aligned} \tag{A.2}$$

(Giuseppe Maria Coclite)
Dipartimento di Meccanica, Matematica e Management, Politecnico di Bari, Via E. Orabona 4,I–70125 Bari, Italy.
*E-mail address*: `giuseppemaria.coclite@poliba.it`
*URL*: `http://www.dm.uniba.it/Members/coclitegm/`

(Giuseppe Florio)
Dipartimento di Meccanica, Matematica e Management, Politecnico di Bari, Via E. Orabona 4,I–70125 Bari, Italy,
INFN, Sezione di Bari, I–70126 Bari, Italy.
*E-mail address*: `giuseppe.florio@ba.infn.it`
*URL*: `https://sites.google.com/site/giuseppefloriomath/`

(Marilena Ligabò)
Dipartimento di Matematica, Università di Bari, Via E. Orabona 4,I–70125 Bari, Italy.
*E-mail address*: `marilena.ligabo@uniba.it`

(Francesco Maddalena)
Dipartimento di Meccanica, Matematica e Management, Politecnico di Bari, Via E. Orabona 4,I–70125 Bari, Italy.
*E-mail address*: `francesco.maddalena@poliba.it`
*URL*: `http://www.dimeg.poliba.it/index.php/it/profilo/userprofile/FMadda`